Theoretical quantification of the electrostatic contribution to complexes involving organolithium compounds

Catherine Fressigné,[a] Jacques Maddaluno[a] and Claude Giessner-Prettre[b] *

[a] *Laboratoire des Fonctions Azotées et Oxygénées Complexes, UPRES-A 6014 CNRS,*
Université de Rouen & IRCOF, 76821 Mont St Aignan Cedex, France
[b] *Laboratoire de Chimie Théorique, UMR 7616 CNRS, Université P. & M. Curie,*
Case Courrier 137, 4 place Jussieu, 75252 Paris Cedex 05, France. E-mail: cgp@lct.jussieu.fr

Received (in Cambridge, UK) 4th March 1999, Accepted 30th July 1999

A quantitative analysis of the intermolecular forces responsible for the formation of aggregates/complexes involving organolithium compounds has been undertaken using the Restricted Variational Space (RVS) decomposition scheme of the intermolecular interaction energy.

Two series of RVS computations have been carried out for every complex. The first one concerns the fully optimized systems while for the second the optimization has been limited to the intermolecular parameters. As expected, our results confirm that the electrostatic contribution is always the main stabilising component in these systems even when one of the partners of the complex is non-polar. In the case of aggregation between two lithiated species, comparison of the two sets of results indicates that the distortion undergone by the partners in the complexes takes place at the expense of an energy decrease of the interacting entities which is minor when compared to the concomitant increase of the electrostatic contribution. In the case of methyllithium dimer we have checked that the extension of the basis set does not alter these results.

Introduction

The efficiency of organolithium compounds in key reactions such as deprotonations or carbon–carbon bond formation endows these reagents with a corner-stone position in organic chemistry. Because of the emphasis put on asymmetric synthesis over the past twenty years, many of these organometallic reagents have been used in conjunction with chiral additives. For alkylation reactions, ligands such as amines,[1] aminoalcohols,[2] alcohols and diols,[2c,3] ethers,[1a,4] aminoethers[5] or oxazolines[6] have been employed, either in stoichiometric or catalytic amounts. Many models have been proposed to justify the enantioselectivities induced by these systems, most of them relying on the putative formation of a tight complex between partners before or during the interaction with the electrophilic species involved in the reaction. Because of their lability, such complexes have been evidenced only in a limited number of cases.[7] More generally, organolithium chemistry is characterized by its tendency to involve clusters presenting polycoordinated lithium atoms, possibly including solvent molecules, and presenting hypervalent-looking carbons, as evidenced both experimentally and theoretically.[7–9] This peculiar behavior has led to detailed theoretical investigations on the nature of the core bonds in various oligomers,[9] Morokuma's energy decomposition scheme[10] being applied even to a set of Li–X dimers such as MeLi and NH_2Li.[9b]

Our recent interest in the field of lithium amide–alkyllithium complexes[7b,8e,11] led us to undertake a quantitative study on the physico-chemical forces driving these molecular phenomena. This investigation has been done using the RVS/CSOV[12] decomposition scheme which provides, like Morokuma's, previously used for the study of methyllithium dimer and smaller entities, an evaluation of the contributions of these different forces to the overall stabilization of the aggregates/complexes studied. In order to encompass as many situations as possible for the different compounds of interest to us, we have considered standard lithiated compounds such as methyllithium (MeLi), lithium dimethylamide (LMA) and lithium ethenolate (CH_2=CHOLi, denoted by EnoLi in the following), taken as models of alkyllithiums, lithium amides and lithium enolates respectively. In the case of EnoLi we have considered two threshold conformations, in agreement with highly accurate *ab initio* calculations,[13] the differences between these two structures possibly altering the stabilization contributions. Interactions between MeLi and dimethyl ether (Me_2O), benzene (C_6H_6) and butyne, and that of LMA with dimethyl ether have also been included in this study in order to examine the contribution(s) which govern(s) the preference between aggregation and complexation. The known importance of the deformation[7–9] undergone by the aggregating species, associated with the alteration of the bonding scheme, prompted us to undertake a second set of calculations corresponding to optimizations limited to the intermolecular geometrical parameters (keeping the internal geometry of the interacting monomers frozen). We thought that the differences between these latter values and those calculated for the fully optimized complex could provide evidence of which contributions are promoted by the monomer distortion.

Computational details

The interaction energy decomposition, which gives access to the electrostatic [E_S], exchange/steric [E_X], polarisation of entity A by the electric field generated by entity B [$E_{pol}(A)$] and charge transfer [E_{ct}] energies, was carried out using the Restricted Variational Space method (RVS)[12a] as implemented in GAMESS.[14] Using the RVS algorithm instead of Morokuma's original analysis[10] offers the advantage that the polarisation and charge transfer contributions of each interacting fragment are calculated separately, as proposed earlier for dimers by the Constrained Space Orbital Variation (CSOV) method.[12b] The geometry optimizations, complete or limited to the intermolecular geometrical parameters (the geometry of the monomers being "frozen") were performed with GAUSSIAN94[15a] at the DFT level only, using the B3P86 functional[16] for consistency with our previous work on this type of

Table 1 Variations of the energy and charges of MeLi with the "extension" of the 6-31G basis set

				6-31G (d,p)	6-31++G (d,p)	6-31G (3df,3pd)	6-31G++G (3df,3pd)
E (a. u)	SCF			−47.0208	−47.0225	−47.0242	−47.0244
	DFT			−47.6140	−47.6162	−47.6183	−47.6181
μ/D	SCF			5.675	5.950	5.740	5.923
	DFT			5.230	5.650	5.397	5.665
Charges	SCF	Li	Mulliken	0.420	0.544	0.397	0.464
			NBO	0.831	0.872	0.834	0.882
		C	Mulliken	−0.616	−0.796	−0.600	−0.778
			NBO	−1.417	−1.423	−1.362	−1.386
		H	Mulliken	0.066	0.084	0.068	0.105
			NBO	0.195	0.184	0.176	0.168
	DFT	Li	Mulliken	0.369	0.553	0.286	0.420
			NBO	0.794	0.854	0.798	0.831
		C	Mulliken	−0.634	−0.907	−0.644	−0.730
			NBO	−1.450	−1.480	−1.416	−1.384
		H	Mulliken	0.088	0.118	0.119	0.103
			NBO	0.219	0.209	0.206	0.168

system.[8e] The basis set used for all the computations was 6-31G**.[17] In the case of methyllithium, the basis set has been progressively enlarged to the 6-31++G(3df,3pd)[17,18] level to investigate the stability of the results with respect to the basis extension. A basis set linear dependency[19] appeared to become of some importance in the case of the largest set. This led us to switch, for the Mulliken populations, to GAUSSIAN98[15b] modifying the threshold value for the elimination of the overlap matrix eigenvalues close to zero (and the corresponding eigenvectors). It also appeared necessary to remove the diffuse s functions on carbon and lithium in order to avoid the occurrence of a spurious population in this orbital (on lithium) when dealing with the 6-31++G(3df,3pd) set. This was not necessary for the NBO charges since this analysis is much less sensitive to near linear dependencies.

Results and discussion

Previous results[9b,c,g,20] have clearly shown the major polar character of lithiated species. The values reported in Table 1 for methyllithium, using the geometry obtained from an optimization carried out with the 6-31G** basis set and the B3P86 functional, confirm these results since the values of the molecular dipole moment (μ) and of the lithium/carbon net charges are large. Table 1 shows also that the molecular energies as well as the charges calculated following the NBO scheme and μ undergo only minor variations upon increasing the size of the basis set from 6-31G** to the more flexible 6-31++G(3df,3pd), and this at the SCF as well as at the DFT levels. The values obtained after a full optimization of MeLi at the DFT level with this latter basis set do not exhibit significant changes compared with the previous ones.

The crucial role played by the electrostatic forces in interactions involving such compounds has been established by a Morokuma intermolecular interaction energy decomposition.[9a] Since we are primarily concerned in this work with such decomposition results, we have checked also that the individual contributions, as well as their variations due to the aggregation-linked distortions, were not modified upon basis set extensions, as shown by the data of Table 2. This observation is in agreement with previous results on smaller basis sets.[9a] These preliminary results indicate that, for such an investigation, the results obtained using the 6-31G** basis set reach a reasonable level of confidence.

Table 2 Variations of the different contributions (in kcal mol^{-1}) to the interaction energy for $(MeLi)_2$ with the "extension" of the 6-31G basis set

	6-31G(d,p)[a]	6-31++G (d,p)	6-31G (3df,3pd)	6-31++G (3df,3pd)[a]
E_S	−99.5 (−49.5)	−101.6	−97.1	−96.7 (−49.1)
E_X	66.2 (34.2)	69.0	66.7	66.1 (34.4)
E_{pol}	−14.4 (−9.4)	−14.0	−17.8	−17.8 (−12.6)
E_{ct}	−6.6 (−4.0)	−6.4	−6.4	−6.0 (−3.4)
ΣE	−54.2 (−28.7)	−53.0	−54.6	−54.2 (−30.7)

[a] Values in parentheses correspond to the frozen geometry situation.

In Table 3 are reported the results concerning aggregates between two organolithium compounds, A and B, of which geometries have been obtained from the two types of optimizations. The first one ("Opt." columns) corresponds to a complete optimization of the complexes, the geometries of the interacting entities obtained from the optimized overall complex being used as input for the RVS computations. Upon the formation of the complex, the monomers A and B get distorted (becoming A′ and B′) and thus A + B→A′–B′. In contrast, the values under the "Froz." headings correspond to the results of optimizations limited to the intermolecular parameters, that is with the internal molecular geometries of A and B as obtained from optimization of the isolated species (A + B→A–B). The ΣE line sums up all the contributions, plus the basis set superposition errors (BSSE, ranging from −0.1 to −1.8 kcal mol^{-1}). It corresponds, except for higher order terms, to the interaction energy between A′ and B′ in the A′–B′ complex for the Opt. columns [$\Sigma E_{opt} = E_{A'-B'} - (E_{A'} + E_{B'})$] and the interaction energy between A and B in the A–B complex for the Froz. columns [$\Sigma E_{froz} = E_{A-B} - (E_A + E_B)$]. The next two lines display, in the Opt. columns, the aggregation energy at the SCF (ΔE_{SCF}) and at the DFT (ΔE_{DFT}) levels, *viz.* $\Delta E = E_{A'-B'} - (E_A + E_B)$. In the Froz. columns, ΔE is equal to $E_{A-B} - (E_A + E_B)$ and differs from ΣE_{froz} only by the higher order terms. The difference between ΔE_{SCF} and ΔE_{DFT} gives an approximation of the dispersion energy. Finally, the last four lines (δE_{SCF} and δE_{DFT}) correspond to the monomer distortion energies upon complexation ($\delta E(A) = E_{A'} - E_A$). The values of these quantities remain similar at the SCF and DFT levels. It is also important to underline that ΔE_{SCF} and ΔE_{DFT} include, in the Opt. columns, both the intermolecular interaction and δE, while the corresponding ΣE values derived from the RVS computations

Table 3 Contributions to the intermolecular interaction energies (kcal mol^{-1}) of optimized complexes containing lithiated species.[a] The "frozen" situation corresponds to a restricted optimization of the complexes (see text)

	$(MeLi)_2$		$(LMA)_2$		MeLi–LMA		EnoLi(I)–LMA		EnoLi(II)–LMA	
	Opt.	Froz.	Opt.	Froz.	Opt.	Froz.	Opt.	Froz.	Opt.	Froz.
E_s	−99.5	−49.5	−112.1	−89.4	−100.3	−68.4	−105.3	−85.5	−96.5	−79.7
E_x	66.2	34.2	60.4	59.0	64.2	45.4	54.0	52.2	49.8	47.5
$E_{pol}(A)$	−7.2	−4.7	−6.2	−5.6	−5.7	−5.1	−5.3	−4.8	−6.7	−5.2
$E_{pol}(B)$	−7.2	−4.7	−6.2	−5.6	−7.6	−5.2	−7.1	−6.8	−6.2	−6.3
$E_{ct}(A)$	−3.3	−2.0	−3.3	−2.4	−2.6	−1.9	−2.2	−2.6	−1.8	−1.4
$E_{ct}(B)$	−3.3	−2.0	−3.3	−2.4	−3.4	−2.5	−3.8	−2.8	−3.4	−2.5
ΣE[b]	−54.2	−28.7	−70.6	−46.4	−55.4	−33.7	−69.7	−50.3	−64.8	−47.6
ΔE_{SCF}[c]	−42.3	−29.2	−61.5	−46.4	−49.0	−38.1	−70.2	−50.8	−65.6	−48.2
ΔE_{DFT}[d]	−44.7[e]	−31.8	−59.7[e]	−49.3	−49.3[e]	−40.3	−61.0	−53.2	−56.8	−49.3
$\delta E_{SCF}(A)$[f]	7.1		6.1		6.5		4.3		2.8	
$\delta E_{SCF}(B)$[f]	7.1		6.1		2.8		5.6		5.2	
$\delta E_{DFT}(A)$[g]	7.0		6.2		6.2		2.4		3.5	
$\delta E_{DFT}(B)$[g]	7.0		6.2		2.2		9.9		5.9	

[a] E_s: electrostatic, E_x: repulsion, E_{pol}: polarisation, E_{ct}: charge transfer. [b] Sum of the different contributions including the basis set superposition errors corrections (BSSE). [c] SCF and [d] DFT interaction energies using the B3P86 geometries. [e] Taken from ref. 10. [f] SCF and [g] DFT energy variation of the monomers due to the geometrical distortion taking place upon the formation of the complex; monomer A is the left part of the AB complex and B the right one.

Table 4 Contributions to the intermolecular interaction energies (kcal mol^{-1}) of optimized complexes containing lithiated species.[a] The "frozen" situation corresponds to a restricted optimization of the complexes (see text)

	MeLi–Me_2O		MeLi–C_6H_6		MeLi–butyne		LMA–Me_2O	
	Opt.	Froz.	Opt.	Froz.	Opt.	Froz.	Opt.	Froz.
E_s	−24.2	−23.0	−9.8	−10.5	−14.2	−12.4	−25.4	−24.9
E_x	9.7	9.2	2.9	5.5	8.7	6.6	10.6	10.3
$E_{pol}(A)$	−0.2	−0.2	−0.5	−0.6	−0.4	−0.3	−0.1	−0.1
$E_{pol}(B)$	−3.7	−3.6	−2.8	−3.7	−3.0	−2.9	−3.8	−4.0
$E_{ct}(A)$	−0.4	−0.4	−0.6	−0.4	−0.3	−0.2	−0.7	−0.6
$E_{ct}(B)$	−0.4	−0.4	−4.4	−2.8	−2.5	−2.4	−0.3	−0.4
ΣE[b]	−19.1	−18.3	−13.2	−12.6	−11.6	−11.5	−19.7	−19.8
ΔE_{SCF}[c]	−19.2	−18.5	−13.1	−12.7	−11.7	−11.6	−19.9	−19.9
ΔE_{DFT}[d]	−19.9	−19.1	−14.8	−14.7	−13.8	−13.5	−20.7[e]	−20.2
$\delta E_{SCF}(A)$[f]	0.0		0.0		0.0		0.1	
$\delta E_{SCF}(B)$[f]	0.1		2.0		0.4		0.2	
$\delta E_{DFT}(A)$[g]	0.0		0.0		0.0		0.1	
$\delta E_{DFT}(B)$[g]	0.4		2.1		0.2		0.4	

[a–g] See footnotes to Table 3.

correspond to the interaction energy between already "distorted" monomers and thus do not take into account the δE.

We see from the values of Table 3 that, in all cases, the electrostatic term (E_S) is by far the main contribution to the stability of the aggregates. The electrostatic factor is 30–45 kcal mol^{-1} larger than the total interaction energy ΣE. This term is however considerably enhanced in the fully optimized (Opt.) complexes when compared to the frozen ones, indicating the importance of monomer distortion for the improvement of the electrostatic interaction. A much more limited increase of the repulsion (E_x) term is observed when going from the frozen to the fully optimized arrangement. The polarization, E_{pol}, and charge transfer, E_{ct}, terms are considerably less modified by the geometrical rearrangements. But the most important feature remains the favorable electrostatic factor that considerably overcomes the unfavorable distortion and exchange destabilizing contributions. The dispersion term is small and even positive in one case. This poor characteristic illustrates the known weakness of many density functionals in accounting for the weak long range van der Waals interactions.[21] Since an accurate evaluation of this term is not relevant to the problem studied here, we choose not to dedicate further attention to this point. Also worthy of note is the variation of ΣE between the two sets of RVS results that reaches, as well as the monomer distortion, a maximum in MeLi and LMA dimers as can be seen from Fig. 1 and Table 3.

Regarding the EnoLi–LMA complexes, it appears that the binding mode of the amide lithium to the oxygen of the enolate's conformation I takes place in a site close to the one occupied by the lithium in conformation II (and *vice versa*) as can be seen from the comparison of Fig. 1D and 1E. A comparable result has been recently reported for enolate dimers.[13b] This binding mode reduces the energy gap between the two complexes with respect to that between the two EnoLi conformations (1.4 and 5.6 kcal mol^{-1} respectively in favor of form II in both cases).

The data of Table 4 deal with complexes between MeLi or LMA and non-lithiated organic molecules, corresponding to solvation-type interactions. The distortions undergone by the monomers in these conditions are much smaller, as can be seen from Fig. 2, than those induced by aggregation phenomena. However, the electrostatics remain the main contributing factor to the overall interaction energy, even with such non-polar compounds as benzene or butyne. In these cases, E_S and ΣE are of the same order of magnitude. The complete optimization of these complexes is associated with only a minor improvement of the interaction energy (<1 kcal mol^{-1}). The gap between the distortion energy values obtained in the present cases and

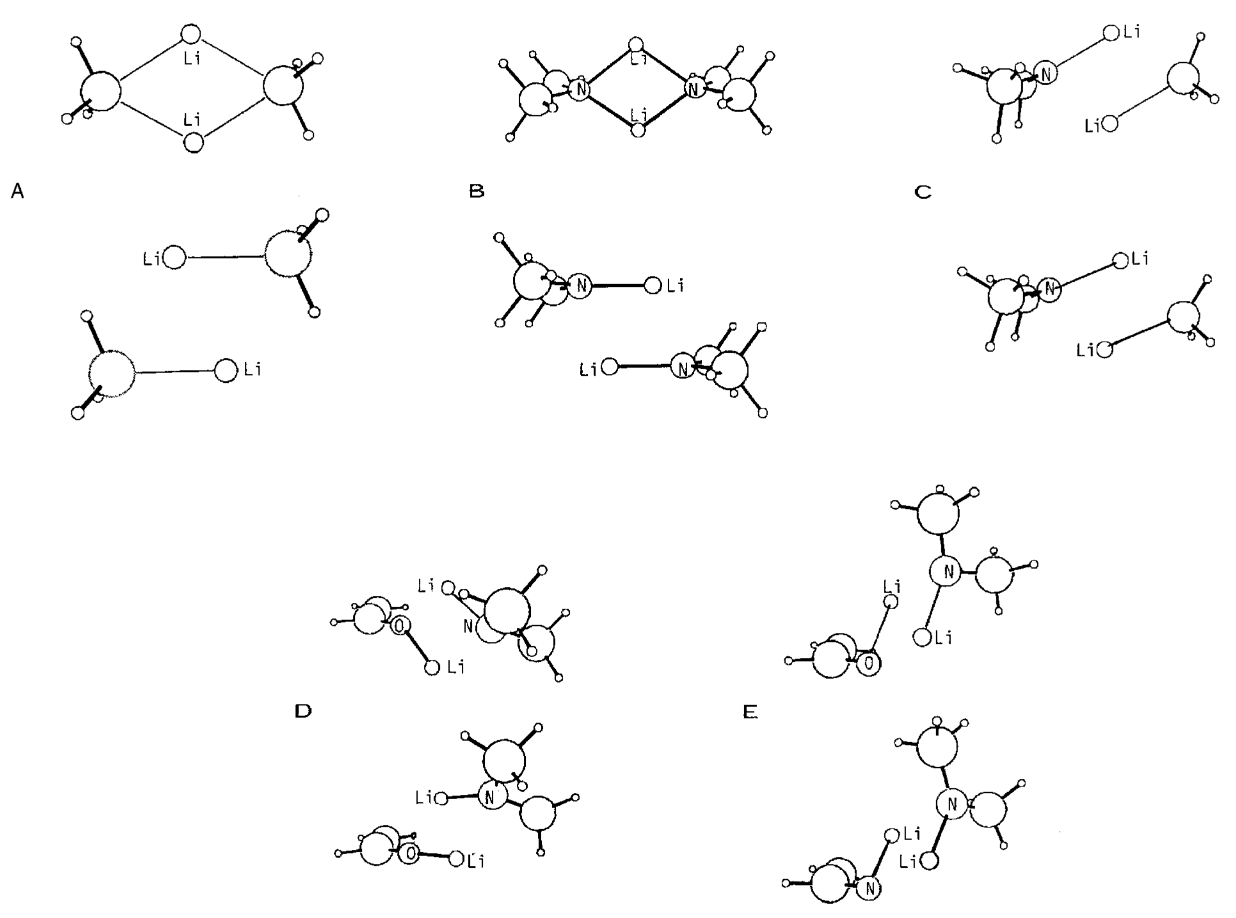

Fig. 1 Optimized arrangements of the complexes between lithiated species (upper: fully optimized complexes; lower: internal geometry frozen): A: $(LiMe)_2$; B: $(LMA)_2$; C: MeLi–LMA; D: EnoLi(I)–LMA; E: EnoLi(II)–LMA.

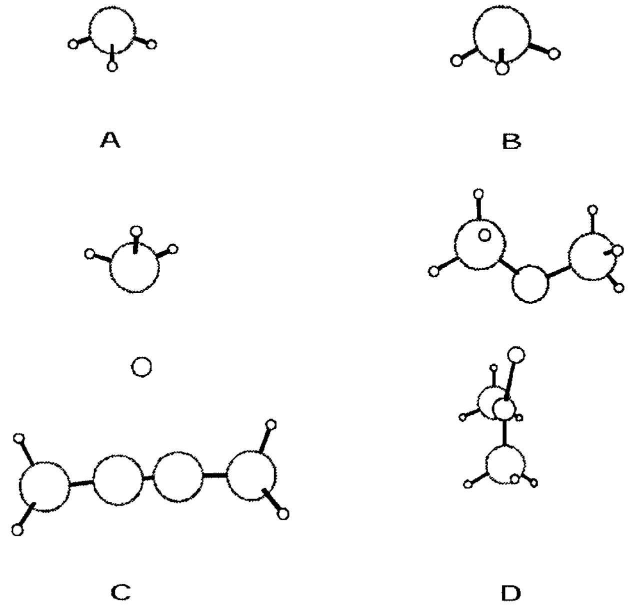

Fig. 2 Optimized arrangements of the complexes between lithiated species and non-lithiated organic molecules. A: MeLi–Me_2O; B: MeLi–C_6H_6; C: MeLi–butyne; D: LMA–Me_2O.

those reported in Table 3 arises from the differences between an interaction inducing a modification of the binding pattern (in the case of lithiated compounds aggregation) and that due to a simple lithium–solvent coordination (Lewis-type neutralization).

The sets of results reported here show that the geometrical distortions taking place upon the formation of organolithium aggregates increase considerably the interaction energy, principally through the electrostatic contribution, at the minor expense of the internal energy of the interacting species. This weak distortion factor is to be related to the well-known low directionality of lithium interactions. The weight of the electrostatic contribution indicates that a strong influence of polar substituents on the interacting partners is to be expected. Last but not least, comparison of the data of Table 3 with those of Table 4 shows that if the monomers were not distorted, the aggregation of MeLi would be disfavored with respect to its complexation in ether (-31.8 *vs.* $-19.9 \times 2 = -39.8$ kcal mol^{-1}). In contrast, in the same conditions LMA would dimerize rather than form a complex with ether (-49.3 *vs.* $-20.2 \times 2 = -40.4$ kcal mol^{-1}) while the mixed dimer MeLi–LMA could be in equilibrium with the MeLi–Me_2O and LMA–Me_2O species (-40.3 *vs.* $-19.1 + -20.2 = -39.3$ kcal mol^{-1}). Similarly MeLi dimer and MeLi–C_6H_6 have comparable stabilities (-31.8 *vs.* $-14.7 \times 2 = -29.4$ kcal mol^{-1}). These concluding remarks could be of interest in relation to the behavior of very rigid lithiated molecules in solution.

Acknowledgements

We thank the Centre de Ressources Informatiques de Haute-Normandie (CRIHAN, Mont Saint Aignan) for computer time within the framework of the "Réseau Normand pour la Modélisation Moléculaire" and Dr A. Savin for helpful discussions.

References

1 *Inter alia*: (*a*) H. Nozaki, T. Aratani and T. Toraya, *Tetrahedron Lett.*, 1968, 4097; (*b*) D. Seebach, H. O. Kalinowski, B. Bastani, G. Grass, H. Daum, H. Dörr, N. P. DuPreez, V. Ehrig, W. Langer, C. Nüssler, H. A. Oei and M. Schmidt, *Helv. Chim. Acta*, 1977, **60**, 301; (*c*) J. P. Mazaleyrat and D. J. Cram, *J. Am. Chem. Soc.*, 1981, **103**, 4585; (*d*) M. B. Eleveld and H. Hogeveen, *Tetrahedron Lett.*, 1984, **25**, 5187; (*e*) M. Nakajima, K. Tomioka and K. Koga, *Tetrahedron*, 1993, **49**, 9751; (*f*) Y. S. Park, M. L. Boys and P. Beak, *J. Am. Chem. Soc.*, 1996, **118**, 3757.

2 *Inter alia*: (*a*) T. Mukaiyama, K. Soai, T. Sato, H. Shimizu and K. Suzuki, *J. Am. Chem. Soc.*, 1979, **101**, 1455; (*b*) L. Colombo, C. Gennari, G. Poli and C. Scolastico, *Tetrahedron*, 1982, **38**, 2725; (*c*) M. Ye, S. Logaraj, L. M. Jackman, K. Hillegass, K. A. Hirsh, A. M. Bollinger and A. L. Grosz, *ibid.*, 1994, **50**, 6109; (*d*) A. S. Thompson, E. G. Corley, M. F. Huntington and E. J. J. Grabowski, *Tetrahedron Lett.*, 1995, **36**, 8937.

3 S. Itsuno, H. Yanaka, C. Hachisuka and K. Ito, *J. Chem. Soc., Perkin Trans. 1*, 1991, 1341.

4 (*a*) D. Seebach and W. Langer, *Helv. Chim. Acta*, 1979, **62**, 1701; (*b*) J. K. Whitesell and B. R. Jaw, *J. Org. Chem.*, 1981, **46**, 2798; (*c*) K. Muruoka and H. Yamamoto, *Angew. Chem., Int. Ed. Engl.*, 1985, **24**, 668; (*d*) K. Tomioka, M. Shindo and K. Koga, *Tetrahedron Lett.*, 1993, **34**, 681.

5 (*a*) K. Tomioka, I. Inoue, M. Shindo and K. Koga, *Tetrahedron Lett.*, 1990, **31**, 6681; (*b*) K. Tomioka, I. Inoue, M. Shindo and K. Koga, *ibid.*, 1991, **32**, 3095; (*c*) I. Inoue, M. Shindo, K. Koga, M. Kanai and K. Tomioka, *Tetrahedron: Asymmetry*, 1995, **6**, 2527.

6 (*a*) S. E. Denmark, N. Nakajima and O. J. C. Nicaise, *J. Am. Chem. Soc.*, 1994, **116**, 8797; (*b*) D. J. Berrisford, *Angew. Chem., Int. Ed. Engl.*, 1995, **34**, 178.

7 Recent examples: (*a*) G. Hilmersson and O. Davidsson, *J. Organomet. Chem.*, 1995, **489**, 175; (*b*) A. Corruble, J. Y. Valnot, J. Maddaluno, Y. Prigent, D. Davoust and P. Duhamel, *J. Am. Chem. Soc.*, 1997, **119**, 10 042; (*c*) P. G. Williard and C. Sun, *ibid.*, 1997, **119**, 11 693; (*d*) A. Thompson, E. G. Corley, M. F. Huntington, E. J. J. Grabowski, J. F. Remenar and D. B. Collum, *ibid.*, 1998, **120**, 2028.

8 *Inter alia*: (*a*) E. Kaufman, P. v. R. Schleyer, K. N. Houk and Y.-D. Wu, *J. Am. Chem. Soc.*, 1985, **107**, 5560; (*b*) R. Glaser and A. Streitwieser Jr, *J. Mol Struct.* (*THEOCHEM*), 1988, **163**, 19; (*c*) R. E. Mulvey, *Chem. Soc. Rev.*, 1991, **20**, 167; (*d*) B. Goldfuss, P. v. R. Schleyer and F. Hampel, *J. Am. Chem. Soc.*, 1997, **119**, 1072; (*e*) C. Fressigné, A. Corruble, J.-Y. Valnot, J. Maddaluno and C. Giessner-Prettre, *J. Organomet. Chem.*, 1997, **549**, 81.

9 *Inter alia*: (*a*) M. Hodoscek and T. Solmajer, *J. Am. Chem. Soc.*, 1984, **106**, 1854; (*b*) P. v. R. Schleyer, *Pure Appl. Chem.*, 1984, **56**, 151; (*c*) E. Kaufmann, T. Clark and P. v. R. Schleyer, *J. Am. Chem. Soc.*, 1984, **106**, 1856; (*d*) E. Kaufman, K. Raghavachari, A. E. Reed and P. v. R. Schleyer, *Organometallics*, 1988, **7**, 1597; (*e*) A. B. Sannigrahi, T. Kar, B. Guha Niyogi, P. Hobza and P. v. R. Schleyer, *Chem. Rev.*, 1990, **90**, 1061; (*f*) L. M. Pratt and I. M. Kahn, *J. Comput. Chem.*, 1995, **16**, 1067; (*g*) F. M. Bickelhaupt, N. J. R. v. Eikema Hommes, C. Foseca Guerra and E. J. Baerends, *Organometallics*, 1996, **15**, 2923; (*h*) R. Gareyev and A. Streitwieser Jr, *J. Org. Chem.*, 1996, **61**, 1742.

10 K. Morokuma, *Acc. Chem. Res.*, 1977, **10**, 294.

11 (*a*) A. Corruble, J. Y. Valnot, J. Maddaluno and P. Duhamel, *Tetrahedron: Asymmetry*, 1997, **8**, 1519; (*b*) A. Corruble, J. Y. Valnot, J. Maddaluno and P. Duhamel, *J. Org. Chem.*, 1998, **63**, 8266.

12 (*a*) W. J. Stevens and W. H. Fink, *Chem. Phys. Lett.*, 1987, **139**, 15; (*b*) P. S. Bagus and C. W. Bauschlicher Jr, *J. Chem. Phys.*, 1984, **80**, 4378.

13 (*a*) H. Weiss, A. V. Yakimansky and A. H. E. Müller, *J. Am. Chem. Soc.*, 1996, **118**, 8897; (*b*) A. Abbotto, A. Streitwieser and P. v. R. Schleyer, *J. Am. Chem. Soc.*, 1997, **119**, 11 255.

14 M. W. Schmidt, K. K. Balridge, J. A. Boatz, S. T. Elbert, M. S. Gordon, J. H. Jensen, S. Koseki, N. Matsunaga, K. A. Nguyen, S. S. Su, T. L. Windus, M. Dupuis and J. A. Montgomery, *J. Comput. Chem.*, 1993, **14**, 1347.

15 (*a*) GAUSSIAN94 (Revision B.1), M. J. Frisch, G. W. Trucks, H. B. Schlegel, P. M. W. Gill, B. G. Johnson, M. A. Robb, J. R. Cheeseman, T. A. Keith, G. A. Petterson, J. A. Montgomery, K. Raghavachari, M.-A. Al-Laham, V. G. Zarzewski, J. V. Ortiz, J. B. Foresman, J. Cioslowski, B. R. Stefanov, A. Nanayakkara, M. Challacombe, C. Y. Peng, P. Y. Ayala, W. Chen, M. W. Wong, J. L. Andres, E. S. Replogle, R. Gomperts, R. L. Martin, D. J. Fox, J. S. Binkley, D. J. Defrees, J. Baker, J. P. Stewart, M. Head-Gordon, C. Gonzales and J. A. Pople, 1995, Gaussian Inc., Pittsburgh, PA; (*b*) GAUSSIAN98 (Revision A5), M. J. Frisch, G. W. Trucks, H. B. Schlegel, G. E. Scuseria, M. A. Robb, J. R. Cheeseman, V. G. Zakrzewfki, J. A. Montgomery, R. E. Stratmann, J. C. Burant, S. Dapprich, J. M. Millam, A. D. Daniels, K. N. Kudin, M. C. Strain, O. Farkas, J. Tomasi, V. Barone, M. Cossi, R. Cammi, B. Mennucci, C. Pomelli, C. Adamo, F. Clifford, J. Ochterski, G. A. Petersson, P. Y. Ayala, Q. Cui, K. Morokuma, D. K. Malick, A. D. Rabuck, K. Raghavachari, J. B. Foresman, J. Cioslowski, J. V. Ortiz, B. B. Stefanov, G. Liu, A. Liashenko, P. Piskorz, I. Komaromi, R. Gomperts, R. L. Martin, D. J. Fox, T. Keith, M. A. Al-Laham, C. Y. Peng, A. Nanayakkara, C. Gonzalez, M. Challacombe, P. M. W. Gill, B. G. Johnson, W. Chen, M. W. Wong, J. L. Andres, M. Head-Gordon, E. S. Replogle and J. A. Pople, 1998, Gaussian Inc., Pittsburgh, PA.

16 (*a*) J. P. Perdew, *Phys. Rev.*, 1986, **B33**, 8822; (*b*) A. D. Becke, *J. Chem. Phys.*, 1989, **90**, 5622.

17 J. M. Frisch, J. A. Pople and J. S. Binkley, *J. Chem. Phys.*, 1984, **80**, 3265.

18 T. Clark, J. Chandrasekhar, G. W. Spitznagel and P. v. R. Schleyer, *J. Comput. Chem.*, 1983, **4**, 294.

19 (*a*) P. S. Bagus and U. I. Wahlgren, *Comput. Chem.*, 1976, **1**, 95; (*b*) A. Szabo and N. Östlund, *Modern Quantum Chemistry*, Dover, New York, 1996, p. 136.

20 *Inter alia*: (*a*) A. Streitwieser Jr, J. E. Williams Jr, S. Alexandratos and J. M. McKelvey, *J. Am. Chem. Soc.*, 1976, **98**, 4778; (*b*) A. B. Sannigrahi, T. Kar, B. Guha Niyogi, P. Hobza and P. v. R. Schleyer, *Chem. Rev.*, 1990, **90**, 1061.

21 (*a*) J. M. Pérez-Jordà and A. D. Becke, *Chem. Phys. Lett.*, 1995, **233**, 134; (*b*) Y. Andersson, D. C. Langreth and B. I. Lundqvist, *Phys. Rev. Lett.*, 1996, **76**, 102.

Paper 9/01731C